

<https://doi.org/10.1038/s41526-025-00468-x>

Brain and cerebrospinal fluid 3D center of mass shift after spaceflight

Check for updates

Katherine G. Warthen¹, Stuart H. Sater¹, Larry A. Kramer², Khader M. Hasan², Michael A. Williams³, Millennia Young⁴, Brandon R. Macias⁴, Steven S. Laurie⁵ & Bryn A. Martin^{1,6,7} ✉

A subset of long-duration spaceflight astronauts at the International Space Station has been documented to develop spaceflight associated neuro-ocular syndrome (SANS). Researchers have sought to understand SANS by quantification of ocular and brain structural changes thought to be associated with weightlessness induced headward fluid shift. Brain tissue shift and cerebrospinal fluid (CSF) redistribution has been observed as measured by MRI on return to Earth, and not fully quantified. To improve the understanding of this phenomenon, we developed and applied automated methods to quantify 3D center of mass shift within the skull of the extra-axial cerebrospinal fluid (eaCSF) and brain after long-duration spaceflight in astronauts ($N = 13$) and controls not exposed to microgravity ($N = 10$). 3D center of mass shift of brain tissue and CSF was computed based on registration of an individual skull segmentation at a baseline timepoint versus follow-up. 3D center of mass shift was quantified in the Gx, Gy, and Gz axis defined as -posterior/+anterior, -left/+right, -inferior/+superior, respectively. For astronauts, average MRI follow-up time pre- to post-flight was 697 ± 137 days (average flight duration = 179 ± 59 days with post-flight MRIs collected an average of 2.23 ± 1.64 days after return to Earth). For controls, average MRI follow-up time was 307 ± 19 days. For astronauts, a superior Gz shift in whole brain was present ($+0.74 \pm 0.28$ mm, $p < 0.0001$) with a concomitant inferior Gz shift in eaCSF (-2.45 ± 0.99 mm, $p < 0.0001$). In the control cohort, brain tissue Gz shift (-0.082 ± 0.048 mm) and eaCSF Gz shift (0.096 ± 0.26 mm) were not statistically significant. Gy shift lacked significance in both controls and astronauts. These findings support that sustained exposure to weightlessness impacts the overall position of fluids and tissues within the skull.

Advances in spaceflight and strides toward long term space habitation are among the most challenging human endeavors of this century. There are a plethora of human health and performance challenges that must be solved before long-term human habitation in space is possible. Long duration spaceflight (LDSF) astronauts (~6 months or greater) experience prolonged time periods without the effect of gravity on the body, which may result in spaceflight associated neuro-ocular syndrome (SANS) among other physical changes. SANS is a syndrome of ocular and brain structural changes including flattening of the posterior ocular globe, choroidal folds, optic disc edema, and minimal brain ventricular enlargement suspected to be related to the redistribution of fluids in the entire body experienced by astronauts during spaceflight^{1–9}. The mechanisms underlying these changes are not yet known.

Investigators have sought to quantify changes in intracranial tissues and fluids during spaceflight that may give clues to understand SANS etiology and lead to potential countermeasures and prognostic indicators. There is evidence of brain volume changes following LDSF, particularly an increase in white matter volume^{2,4,9–15}. Koppelmans et al. hypothesized that macroscopic decrease in gray matter volume may be due to sensorimotor adaptations during spaceflight¹¹. Significant regional changes in free water volume and white matter diffusion were found by Lee et al.². Changes in intracranial CSF have been documented, with most studies highlighting ventricular enlargement^{1,4,9,10,13,14,16–18}. Ventricular enlargement was found to depend on flight duration, with longer flight times leading to greater volume increase¹. CSF space thinning near the cranial vertex has been documented in astronauts post flight^{2,7,12}. CSF dilation in the perivascular spaces of the brain has also been demonstrated^{12,18,19}. Aqueductal CSF stroke volume and

¹Alcyone Therapeutics Inc, Lowell, MA, USA. ²McGovern Medical School at UTHealth Houston, Houston, TX, USA. ³University of Washington School of Medicine, Seattle, WA, USA. ⁴NASA, Houston, TX, USA. ⁵KBR, Houston, TX, USA. ⁶Dept. of Chemical and Biological Engineering, University of Idaho, Moscow, ID, USA. ⁷Flux Neuroscience, LLC, Troy, ID, USA. ✉e-mail: bryn@alcyonetx.com

velocity were found by Kramer et al. to increase in astronauts post-flight compared to pre-flight and hypothesized to be associated with altered intracranial compliance due to whole brain and ventricular expansion⁴. Kramer et al. also found a rebound increase in postflight CSF production rate for astronauts with posterior optic globe flattening and speculated that this was in response to an inflight downregulation of CSF production rate associated with microgravity-induced intracranial hypertension²⁰. Headward fluid shift during spaceflight has also been noted to cause jugular vein distension and retrograde flow²¹, with a recent jugular vein thrombosis observed via ultrasound²². In combination, these studies support that spaceflight may alter the complex relation of intracranial tissues and fluids at both the macro- and microscale.

As evident as the structural and volumetric changes detailed above appear to be, how prolonged exposure to microgravity affects position of the brain and the distribution of the surrounding CSF, has not been fully quantified. Relative change in the position of the brain within the skull was first identified in astronauts by visual inspection of magnetic resonance imaging (MRI)⁷. The vertical component of brain displacement was estimated by visual alignment and comparison of pre-versus post-flight MRI collected for 18 long-duration and 16 short-duration astronauts. Greater brain displacement was observed in long-duration spaceflight astronauts compared to short-duration. These results have been replicated by several authors^{1,2,10,11,17}.

Quantification is needed to understand the 3-dimensional extent of brain shift within the skull and its relation, if any, to intracranial CSF shift. We developed and implemented a novel automated method to quantify white matter, gray matter, blood, lateral ventricle CSF, extra-axial CSF (eaCSF), and 3D center of mass position change, or “shift”, with respect to the entire skull. The center of mass is used as an indicator of 3D shift as it integrates the overall changes taking place for each region of interest, with all parts of the region being taken into account rather than looking at local changes (e.g. thinning of the eaCSF near the vertex). We use a skull only rigid-body registration to provide a consistent reference that is unlikely to change over spaceflight. Evaluating CSF shift in combination with brain shift gives a more complete understanding of the 3D changes within the cranial vault and the opportunity to explore their potential interactions. As this is a rigid-body approach, we do not venture to describe the deformations of the brain tissue, which should be explored in further studies and is of utmost importance for full understanding of the phenomenon. We propose this method as a reliable summary of the motion of tissues and fluids within the intracranial cavity. In this case-control study, a control cohort that did not embark in spaceflight was scanned on the same MRI as the astronaut group and had a similar MRI follow-up duration. Including controls allows for changes in the center of mass to be interpreted relative to the aging process and other sources of normal variation. We hypothesized that there would be a caudocranial directed superior shift of the brain center of mass and a corresponding craniocaudal inferior shift, or redistribution, of eaCSF after spaceflight that would not occur in control participants.

Results

Subjects

Final analyses included 10 astronauts (2 female) of mean \pm standard deviation (SD) age 46.4 ± 5.99 years. Average time in space was 159 ± 59 days and imaging was performed an average of 2.23 ± 1.64 days after return to Earth. For controls, average MRI follow-up time was 307 ± 19 days. Seven control participants were included (4 female), of mean age 38.9 ± 7.33 years.

Tissue and Fluid 3D Shifts

Tissue and fluid shift was mainly found in the Gz (- inferior / + superior) and Gx (- posterior / + anterior) axes (Fig. 1A). The magnitude of change in each axis for each variable by group is shown in Table 1, and an example visualization of extent of brain shift is shown in Fig. 2A–C and Supplementary Video 1. With respect to the brain, astronauts demonstrated a superior Gz shift in white matter center of mass versus controls (0.74 ± 0.28 mm vs. -0.12 ± 0.07 mm, $p < 0.0001$), but there was no difference in Gx shift between groups (Table 1). The superior Gz shift in grey matter in astronauts was greater than controls (0.57 ± 0.34 mm vs. -0.07 ± 0.04 mm, $p < 0.0001$), with no Gx shift between groups (Table 1). Similarly, the superior Gz shift in whole brain in astronauts was greater than controls (0.63 ± 0.32 mm vs. -0.08 ± 0.05 mm, $p < 0.0001$), and not different in Gx shift (Fig. 3A, Table 1).

In the lateral ventricle CSF, no change was found in Gz shift but a Gx shift in the lateral ventricle CSF was found in astronauts versus controls (0.63 ± 0.77 mm vs. 0.02 ± 0.24 mm, $p = 0.017$) (Fig. 3B, Table 1). The eaCSF segmentation had greater inferior Gz shift in astronauts versus controls (2.45 ± 0.99 mm vs. 0.10 ± 0.26 mm, $p < 0.0001$) and anterior Gx shift (1.09 ± 0.67 mm vs. 0.23 ± 0.71 mm, $p = 0.019$) (Fig. 3C, Table 1). The degree of eaCSF shift was quite apparent in astronauts, with inferior Gz shift up to nearly -4 mm and anterior Gx shift up to nearly 2 mm (Fig. 3D). A small right Gy shift in total intracranial blood was found in astronauts versus controls (0.38 ± 0.19 vs. 0.084 ± 0.39 , $p = 0.0044$). Gz and Gx shift in total intracranial blood did not differ between groups.

Tissue and Fluid Volume Changes

Total gray matter volume increased in astronauts but not in controls (5.67 ± 6.63 cm³ vs. -1.69 ± 1.79 cm³, $p = 0.0041$) (Table 1). However, white matter volume, whole brain volume, and total intracranial volume change was not significant (Fig. 4A, Table 1). Total intracranial CSF volume decreased in astronauts versus controls (-3.73 ± 5.93 cm³ vs. 3.26 ± 1.51 cm³, $p = 0.001$) (Table 1), while ventricle volume increased in astronauts compared to controls (2.63 ± 2.18 cm³ vs. 0.04 ± 0.33 cm³, $p = 0.0086$) (Fig. 4B). EaCSF volume decreased in astronauts versus controls (-6.49 ± 6.3 cm³ vs. 3.45 ± 1.61 cm³, $p < 0.0001$) (Fig. 4C). Total volumes are included in Supplementary Table 1. Average total intracranial volume change was 3.4 ± 9.1 cm³, or 0.22%, in the combined cohort of astronauts and controls and not statistically different between groups, likely representing a measure of error in the segmentations as the Monro-Kellie doctrine²³ would predict a 0% change.

Fig. 1 | Visualization of shift axis and sign indication on a template MNI brain. A Gz axis indicating shift in the inferior (–) or superior (+) axis. Gx axis indicating shift in the posterior (–) or anterior (+) axis, and **B** 3D visualization of a CSF segmentation after McRae crop overlaid on the original image.

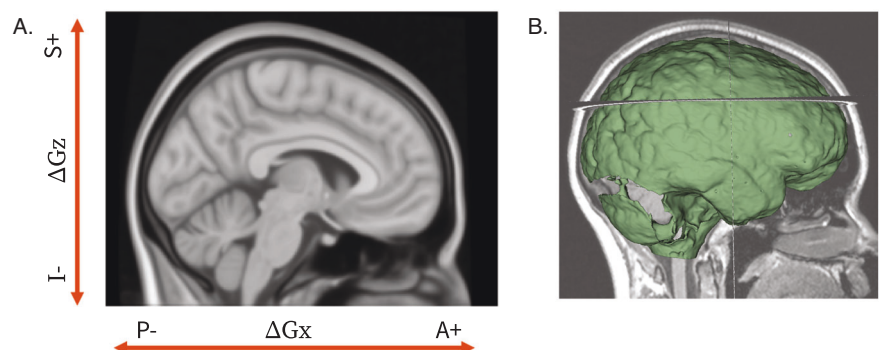


Table 1 | Change in center of mass in Gx, Gy, and Gz axis and volume change from baseline for each variable

	LDSF Astronauts	Controls	
Gz shift	mean ± SD (mm)	mean ± SD (mm)	Comparison of change, LDSF Astronauts vs. Controls
White Matter	0.74 ± 0.28	−0.12 ± 0.07	<0.0001
Gray Matter	0.57 ± 0.34	−0.07 ± 0.04	<0.0001
Whole Brain	0.63 ± 0.32	−0.08 ± 0.05	<0.0001
Intracranial CSF	−2.14 ± 0.83	0.12 ± 0.23	<0.0001
Intracranial Blood	−0.48 ± 1.66	−0.87 ± 0.96	0.5357
Lateral Ventricle	0.31 ± 0.52	−0.01 ± 0.21	0.0858
eaCSF	−2.45 ± 0.99	0.096 ± 0.26	<0.0001
Gx shift	mean ± SD (mm)	mean ± SD (mm)	Comparison of change, LDSF Astronauts vs. Controls
White Matter	−0.15 ± 0.27	−0.002 ± 0.09	0.1132
Gray Matter	−0.16 ± 0.18	−0.08 ± 0.20	0.3764
Whole Brain	−0.16 ± 0.20	−0.05 ± 0.15	0.2052
Intracranial CSF	0.93 ± 0.60	0.23 ± 0.66	0.0294
Intracranial Blood	−0.27 ± 1.32	−0.29 ± 0.51	0.9921
Lateral Ventricle	−0.63 ± 0.77	0.02 ± 0.24	0.0168
eaCSF	1.09 ± 0.67	0.23 ± 0.71	0.0194
Gy shift	mean ± SD (mm)	mean ± SD (mm)	Comparison of change, LDSF Astronauts vs. Controls
White Matter	0.21 ± 0.60	0.035 ± 0.06	0.3404
Gray Matter	0.034 ± 0.07	0.02 ± 0.06	0.563
Whole Brain	0.022 ± 0.06	0.023 ± 0.06	0.9775
Intracranial CSF	−0.12 ± 0.17	−0.073 ± 0.13	0.5167
Intracranial Blood	0.38 ± 0.19	−0.084 ± 0.39	0.0044
Lateral Ventricle	−0.081 ± 0.26	−0.018 ± 0.13	0.5042
eaCSF	−0.14 ± 0.16	−0.079 ± 0.15	0.3951
Volume change	mean ± SD (cm³)	mean ± SD (cm³)	Comparison of change, LDSF Astronauts vs. Controls
White Matter	3.39 ± 9.46	0.25 ± 4.72	0.437
Gray Matter	5.67 ± 6.63	−1.69 ± 1.79	0.0041
Whole Brain	9.06 ± 15.05	−1.43 ± 5.82	0.0644
Intracranial CSF	−3.73 ± 5.93	3.26 ± 1.51	0.001
Intracranial Blood	−0.55 ± 0.69	−0.47 ± 0.96	0.9549
Lateral Ventricle	2.63 ± 2.18	0.04 ± 0.33	0.0086
eaCSF	−6.49 ± 6.30	3.45 ± 1.61	<0.0001

Bold values indicate where a change was significantly different between groups

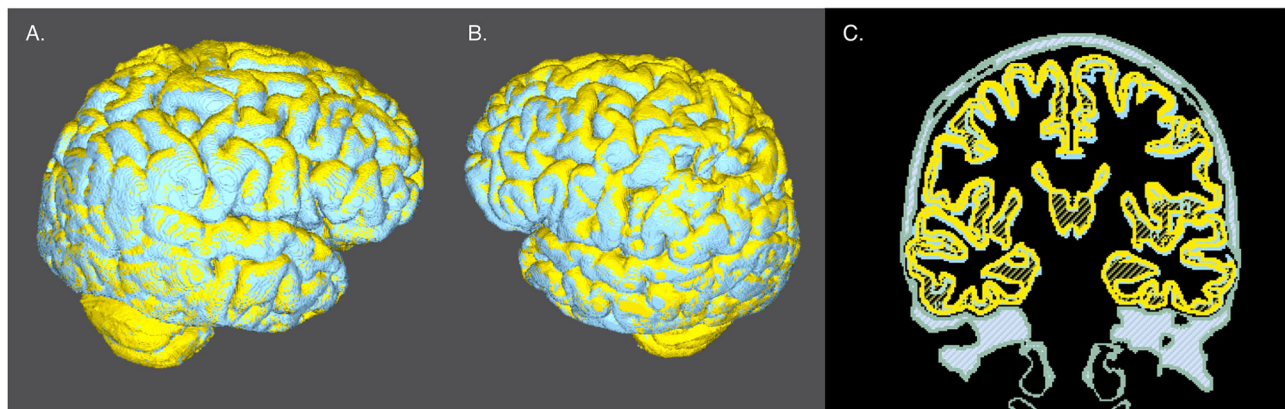


Fig. 2 | 3D visualization of upward brain center of mass shift for a specific astronaut. A and B yellow represents a post-flight brain and blue represents pre-flight, and **C** Coronal slice visualization of brain shift overlaid with skull bone

shown in grey hatching. Pixels shown are not necessarily the original image voxel size but are due to the 3D image visualization software processing. (see also Supplementary Video 1).

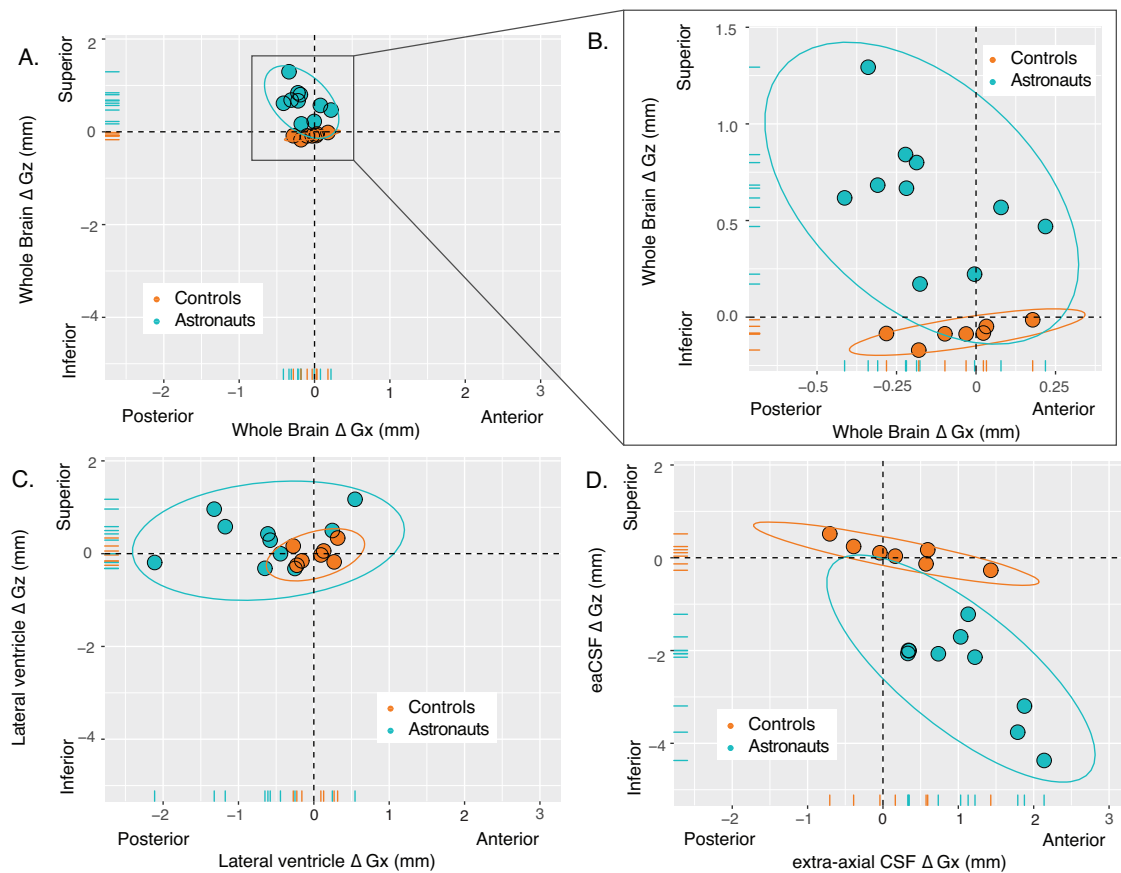


Fig. 3 | Shift by center of mass. **A** Whole brain shift in the Gz and Gx axis for astronauts (blue) and controls (orange), **B** Zoom view of whole brain shift showing consistently greater Gz axis shift in astronauts compared to controls, **C** Lateral ventricle shift, and **D** eaCSF shift (total CSF – lateral ventricles). Ellipses around each group represent the 95% confidence interval.

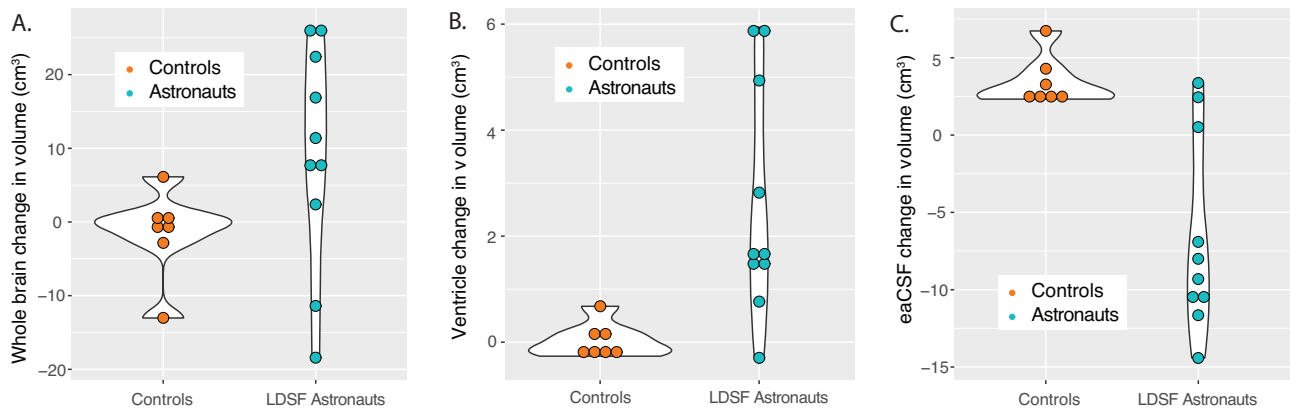


Fig. 4 | Volume changes for each timepoint vs. baseline. **A** Whole brain change in volume, (12 mo controls: orange, astronauts: blue) **B** Lateral ventricles, and **C** EaCSF (extra-axial CSF: total CSF – lateral ventricles).

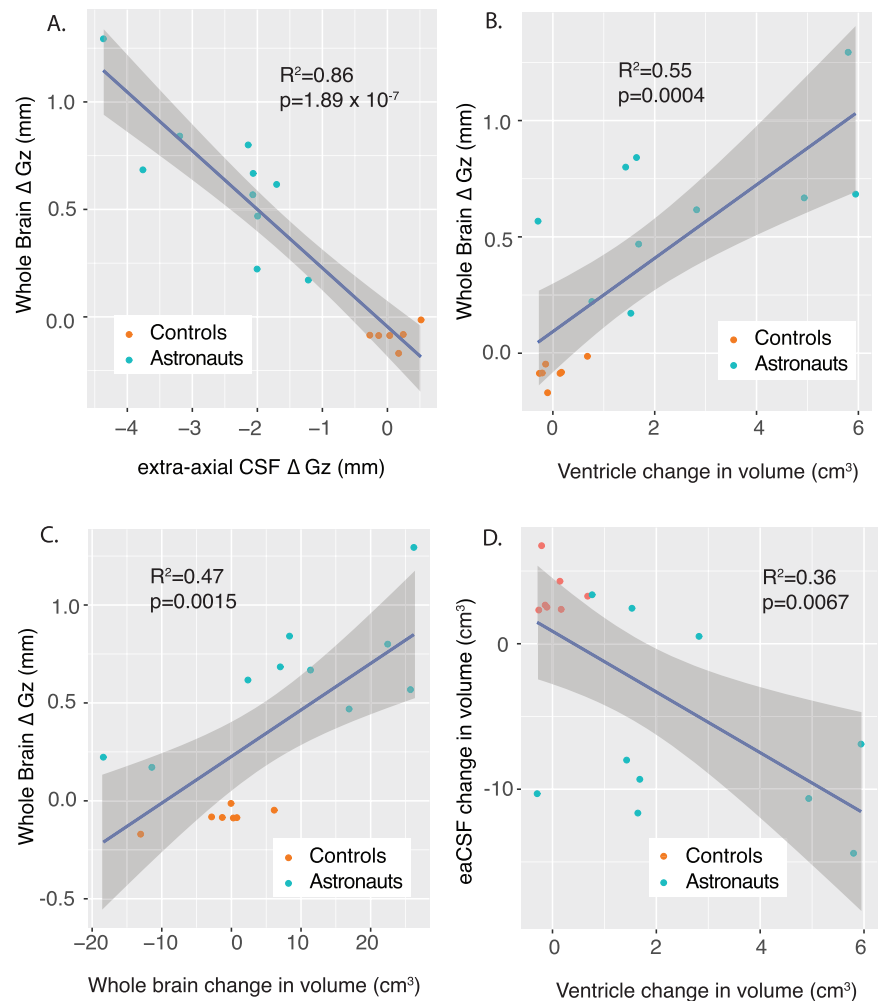
Correlation of Shift and Volume Change

In the combined group, whole brain Gz shift and eaCSF Gz shift were strongly anticorrelated, indicating that the superior shift of the brain coincided with inferior redistribution of eaCSF that was in the opposite direction ($R^2 = 0.86$, $p = 1.89 \times 10^{-7}$) (Fig. 5A). Ventricle CSF volume change was correlated with whole brain shift ($R^2 = 0.55$, $p = 0.0004$) (Fig. 5B), and whole brain volume change correlated significantly with whole brain superior Gz shift ($R^2 = 0.47$, $p = 0.0015$) (Fig. 5C). Change in volume of the eaCSF was inversely correlated with the change in volume of the ventricles ($R^2 = 0.36$, $p = 0.0067$) (Fig. 5D).

Discussion

We developed a novel approach to objectively quantify shifts in the center of mass of brain tissue and CSF and applied this analysis to MR images acquired in astronauts following long-duration spaceflight and compared to ground-based controls. Our results demonstrate significant change in brain center of mass along with significant eaCSF redistribution as demonstrated by change in center of mass in astronauts, and as expected, no change in controls. By using the same scanner and the same sequences for astronauts and controls as well as quantifying the entire eaCSF region, we are in a better position to confirm that the changes seen in astronauts are related to the

Fig. 5 | Pearson linear correlations for the combined groups. Correlations between whole brain Gz shift and A eaCSF Gz shift, B lateral ventricle change in volume, and C whole brain change in volume, as well as D eaCSF change in volume and ventricle change in volume. Shaded region represents the 95% confidence interval.



effect of LDSF on brain and CSF physiology and not potentially due to scanner related variability thereby allowing greater confidence in the findings. By quantifying the entire eaCSF region in combination with the brain, we can deduce a wholistic view of intracranial fluid redistribution that may occur due to spaceflight.

Unsurprisingly, there was nearly zero shift in whole brain or eaCSF in controls. In contrast, whole brain superior Gz shift (~ 0.6 mm) and inferior eaCSF Gz redistribution (~ 2.5 mm) was significant in astronauts (Table 1). Based on the individual data points, there was no overlap in this finding between groups (Figs. 3D and D). The superior whole brain Gz shift had a strong anticorrelation with an inferior eaCSF Gz shift (Fig. 5A, $R^2=0.86$, $p=1.89 \times 10^{-7}$). While ventricular volume increase was present in astronauts, the majority of CSF shift occurred within the eaCSF. Ventricle volume increase was moderately correlated with superior whole brain Gz shift (Fig. 5B, $R^2=0.55$, $p=0.0004$), and whole brain volume increase was moderately correlated with superior whole brain Gz shift (Fig. 5C, $R^2=0.47$, $p=0.0015$). Volume change in the eaCSF was moderately anticorrelated with volume change in the lateral ventricles (Fig. 5D, $R^2=0.36$, $p=0.0067$).

Whole brain superior Gz shift appears to be greater near the cranial vertex than the skull base (Fig. 2C), indicating a brain stretch rather than a uniform brain shift as quantified in the current study. A non-uniform brain stretch would potentially require non-homogenous changes in regional brain volume^{15,17}. Increased volume in the motor cortex in the superior regions has been observed with astronaut adaptation to spaceflight¹⁵ which could produce some change in center of mass, however this would not account for the total brain shift observed. Deformation analyses are necessary to understand how localized brain morphology factors such as

these may be impacted by LDSF. Future studies must be conducted on detailed brain morphology to fully understand these changes in the system, and whether or not they relate to cognition, cellular morphology, or other central nervous system changes observed in spaceflight²⁴. Center of mass shift should be interpreted as a summary of the changes in a system, not a detailed account. The center of mass in mm space is determined based on the weighted contribution of all voxels, thus the resulting center of mass is not restricted to discrete voxel locations but represents an average position in continuous space. Further factors that could have an impact on these results include hydration status²⁵, which may impact volume of brain structures, and relative pulsatility of the brain²⁶, which if accounted for may provide a more accurate volume and position measure.

The anticorrelation of eaCSF shift to brain shift indicates that the eaCSF shift could be a compensatory response to brain movement. The center of mass change of the CSF represents a redistribution of fluid, as opposed to the movement of a solid mass, such as the brain, as discussed by Lee et al.² and Koppelmans et al.¹¹. The eaCSF center of mass shift magnitude is greater than the brain tissue shift because of its fluid geometry that is roughly a hollow shell where a small movement of the interior spherical shaped brain can produce a large redistribution of eaCSF around the brain which results in the change in center of mass. For this reason, greater change in eaCSF versus brain center of mass does not imply that eaCSF volume movement around the brain is greater. Additionally, we observed a decrease in eaCSF volume and a similar increase in total brain volume. The increase in brain volume may be partially accounted for by the expansion of perivascular spaces, as shown by Barisano et al.¹², although our study did not specifically compute perivascular space volume change.

Although we did not measure this directly, a potential consequence of brain shift in the superior Gz axis may be decreased eaCSF space near the vertex, as previously documented by several studies^{7,12}. In the present study, we also demonstrated an anterior eaCSF center of mass shift toward the cavernous sinus and the optic bulbar sub-arachnoid space, potentially altering the local CSF pulsatility that could act on the optic nerve, nerve head, and posterior optic globe²⁷. The correlation and mechanistic linkage, if any, between SANS ocular changes and brain shift or volume change remains to be quantified. A thinned or thickened eaCSF layer between the skull and brain may also alter the intracranial fluid pressure dynamics that occur with each cardiac-induced CSF oscillation. We also observed a decrease in eaCSF volume that coincided with an increase in whole brain volume (Table 1). In combination, these changes would decrease intracranial compliance and increase intracranial CSF pulsatility, but these changes may not impact mean intracranial pressure. Further studies should examine alterations in eaCSF near the cranial base and more specifically, cavernous sinus, as this region is closely coupled to the arterial source of intracranial pulsatility. We did not account for CSF redistribution into the spinal subarachnoid space, which could be investigated in future work.

Along with spaceflight application, a potential clinical application of the 3D center of mass shift methods presented is spontaneous intracranial hypotension, for which brain imaging is currently assessed either subjectively or by the Bern scale²⁸. Application of this method could help determine if the clinical treatment in fact restores the intracranial contents to their normal position within the cranial vault.

Changes in intracranial tissue and fluid volume and shift were measured approximately 3 days post-flight, but it is not known how long these alterations persist after return to Earth. The measures provided here represent the sum of all brain tissue and CSF movement and do not capture or quantify the brain tissue morphological changes that have been observed to differ between brain regions. These results should be replicated in a larger cohort, with all available astronaut data and related head down tilt studies for an earth-bound analog study. Researchers were not blinded to the participant status of control versus astronaut. It would be advantageous to correlate these findings in the future with optic globe changes and other SANS structural changes, as well as how time in space impacts the extent of brain shift, and to explore the brain more granularly through regional or whole brain deformation approaches. Other factors related to brain shift such as intracranial pressure and tissue compliance should be further explored.

We observed a superior brain shift in center of mass and anterior and inferior extra-axial redistribution of CSF in astronauts following long-duration spaceflight based on objective quantification of MR images. The brain shift and CSF redistribution findings were consistent for every astronaut in the study cohort. We also observed that the degree of shift may not occur equally throughout the brain, highlighting the need to better assess morphological changes to fully understand spaceflight-induced structural changes. Future studies are needed to elucidate the driving mechanisms that promote intracranial shift and determine whether these changes relate to alteration of cerebral function and other observed changes in the central nervous system.

Methods

This longitudinal case control study included a cohort of LDSF astronauts and ground-based control participants. Written informed consent was obtained from all participants in accordance with NASA IRB guidelines.

Timeline

MRI scans were performed on LDSF astronauts ($n = 13$) before and 2.23 ± 1.64 days after return to Earth (Return + 3 days, R + 3) following 179 ± 59 days in space (mean \pm SD). The terrestrial control cohort ($n = 10$) underwent MRI collection at baseline and a 12-month follow-up timepoint (366 ± 15 days) on the same MR scanner as the LDSF astronauts.

MRI Collection, Segmentation, and Registration

A series of T1-weighted images with full brain coverage were collected on a Siemens 3 T MR scanner (Verio 3 T; vB19; Siemens Healthineers, Erlangen, Germany) for both cohorts with a 3D Turbo-FLASH sequence, 256×256 mm FOV, 512 columns \times 512 rows \times 176 slices, voxel size (0.49 mm, 0.49 mm, 0.9 mm), repetition time TR = 1900 ms, echo time TE = 2.32 ms, and 9° flip angle, and gradient 45 mT/m at 200 T/ms with a full body coil.

Each image was aligned via multiplanar reslicing so that the anterior-posterior and left-right fields of view were positioned on the same plane using the longitudinal fissure as a reference and the anterior-posterior crosshairs for alignment. Similarly, the inferior-superior (top-bottom) and left-right fields of view were also aligned using the longitudinal fissure, guided by the inferior-superior crosshairs. The McRae line²⁹ was then determined as defined above at the base of the skull and the corresponding plane was used to crop the image (Fig. 1B) to include only intracranial tissues. The cropped images were segmented with Charn³⁰ into the individual components of total gray matter, white, matter intracranial CSF (combined lateral ventricles and extra-axial CSF), blood, and skull. Brain volume analyses were performed in subject specific imaging space, where “post” images were registered to baseline images with skull segmentation only with a rigid body registration (SPM12³¹). Skull registration quality was checked with the Sørensen-Dice coefficient calculated in 3D Slicer³² where values greater than 0.8 were considered acceptable. The Sørensen-Dice coefficient provides a measure of the ratio of common elements in two images, here we use this to determine that the skull segmentations are sufficiently overlapped to ensure correct registration. In addition to Sørensen-Dice coefficient quality control, a single expert operator visually inspected each brain segmentation as an additional step to verify segmentation robustness.

Data Analysis

3D center of mass was defined as a unique point where the weighted relative position of the distributed mass sums to zero³³. At this unique point, the entire mass of a 3D object can be concentrated, and a force can be applied to cause linear acceleration without angular acceleration. 3D center of mass change in position, referred to as “shift” throughout this manuscript, was defined as the 3D vector connecting the center of mass point at baseline compared to follow-up with a vector coordinate system defined by the axes used in gravitational physiology with -Gy left, +Gy right, -Gx posterior, +Gx anterior, -Gz inferior, and +Gz superior³⁴. For the purposes of this analysis, all tissues and fluids are assumed to have uniform density.

3D Center of mass shift (in mm) and volume change (in cm^3) from baseline was calculated for white matter, gray matter, whole brain (white matter + gray matter) total intracranial CSF, lateral ventricles, eaCSF defined as the total intracranial CSF segmentation minus lateral ventricle segmentation, and total intracranial blood. Volume and center of mass were both calculated with FSL³⁵, and volume and shift figures were produced using R³⁶ (4.2.0) with ggplot2³⁷. Brain visualizations were produced in Seg3D³⁸. According to the Monro-Kellie doctrine²³, accurate segmentations are presumed to find zero total intracranial volume change between time-points. Thus, the total intracranial volume change for each subject was calculated to confirm this conservation principle.

Each variable was analyzed in separate generalized linear mixed models defined in terms of the interaction between group (Astronaut or Control) and time (pre or post). This ANOVA model specified a mean value to each category combination. Subject-specific random intercepts addressed the repeated measures within individuals and robust standard errors allowed for non-homogenous variance. The marginal means were used for estimation and pairwise comparisons. If the overall F-test for the interaction was significant, pairwise comparisons included between groups at each timepoint, the pre to post change within groups, and contrasts of those changes between groups. The primary focus of testing was on contrasting the pre to post changes between groups. Residuals were examined to ensure conformation to the normality assumption. Volume measures achieved improved residual normality through using a natural log link function in the

generalized linear models ($\ln(\mu) = \text{Group} * \text{Time}$). Gx, Gy, and Gz axis measures used the typical identity link $\mu = \text{Group} * \text{Time}$. Simulation based p-value adjustments were used to address the multiple testing within each model. These analyses were run in SAS v9.4 using the GLIMMIX procedure. In the results, we report the mean changes \pm SD of the raw data with p-values from the model-based comparisons.

To further analyze associations between measures, exploratory Pearson linear regressions between the pre to post changes of specific brain variables, including whole brain Gz shift, eaCSF Gz shift, lateral ventricle change in volume, and whole brain change in volume, were conducted. Estimates of correlation along with model fit predictions were conducted and visualized using R³⁶ (4.2.0). Group status was ignored for these estimates.

Data availability

Data from this study may be obtained through a data request to the NASA LifeScience Data Archive.

Code availability

Code will be made available upon request from the authors.

Received: 28 May 2024; Accepted: 18 March 2025;

Published online: 08 May 2025

References

- Hupfeld, K. E. et al. The Impact of 6 and 12 Months in Space on Human Brain Structure and Intracranial Fluid Shifts. *Cereb. Cortex Commun.* **1**, 1–15 (2020).
- Lee, J. K. et al. Spaceflight-Associated Brain White Matter Microstructural Changes and Intracranial Fluid Redistribution. *JAMA Neurol.* **76**, 412–419 (2019).
- Macias, B. R. et al. Association of Long-Duration Spaceflight With Anterior and Posterior Ocular Structure Changes in Astronauts and Their Recovery. *JAMA Ophthalmol.* **138**, 1–7 (2020).
- Kramer, L. A. et al. Intracranial Effects of Microgravity: A Prospective Longitudinal MRI Study. *Radiology* **295**, 640–648 (2020).
- Sater, S. H. et al. Automated MRI-based quantification of posterior ocular globe flattening and recovery after long-duration spaceflight. *Eye (Lond.)* **35**, 1869–1878 (2021).
- Ferguson, C. R. et al. Incidence and Progression of Choriorretinal Folds During Long-Duration Spaceflight. *JAMA Ophthalmol.* **141**, 168–175 (2023).
- Roberts, D. R. et al. Effects of Spaceflight on Astronaut Brain Structure as Indicated on MRI. *N. Engl. J. Med.* **377**, 1746–1753 (2017).
- Jillings, S. et al. Macro- and microstructural changes in cosmonauts' brains after long-duration spaceflight. *Sci. Adv.* **6**, eaaz9488 (2020).
- Van Ombergen, A. et al. Brain Tissue-Volume Changes in Cosmonauts. *N. Engl. J. Med.* **379**, 1678–1680 (2018).
- McGregor, H. R. et al. Impacts of spaceflight experience on human brain structure. *Sci. Rep.* **13**, 7878 (2023).
- Koppelmans, V., Bloomberg, J. J., Mulavara, A. P. & Seidler, R. D. Brain structural plasticity with spaceflight. *npj Microgravity* **2**, 1–8 (2016).
- Barisano, G. et al. The effect of prolonged spaceflight on cerebrospinal fluid and perivascular spaces of astronauts and cosmonauts. *Proc. Natl. Acad. Sci. USA* **119**, e2120439119 (2022).
- Hasan, K. M. et al. Brain Quantitative MRI Metrics in Astronauts as a Unique Professional Group. *J. Neuroimag.* **28**, 256–268 (2018).
- Riascos, R. F. et al. Longitudinal Analysis of Quantitative Brain MRI in Astronauts Following Microgravity Exposure. *J. Neuroimag.* **29**, 323–330 (2019).
- Koppelmans, V. et al. Cortical thickness of primary motor and vestibular brain regions predicts recovery from fall and balance directly after spaceflight. *Brain Struct. Funct.* **227**, 2073–2086 (2022).
- Roberts, D. R. et al. Longitudinal change in ventricular volume is accelerated in astronauts undergoing long-duration spaceflight. *Aging Brain* **1**, 100017 (2021).
- Van Ombergen, A. et al. Brain ventricular volume changes induced by long-duration spaceflight. *Proc. Natl. Acad. Sci.* **116**, 10531–10536 (2019).
- Alperin, N., Bagci, A. M. & Lee, S. H. Spaceflight-induced changes in white matter hyperintensity burden in astronauts. *Neurology* **89**, 2187–2191 (2017).
- Hupfeld, K. E. et al. Longitudinal MRI-visible perivascular space (PVS) changes with long-duration spaceflight. *Sci. Rep.* **12**, 7238 (2022).
- Kramer, L. A. et al. MR-derived cerebral spinal fluid hydrodynamics as a marker and a risk factor for intracranial hypertension in astronauts exposed to microgravity. *J. Magn. Reson Imaging* **42**, 1560–1571 (2015).
- Marshall-Goebel, K. et al. Jugular venous flow dynamics during acute weightlessness. *J. Appl. Physiol.* (1985) **136**, 1105–1112 (2024).
- Pavella, J. et al. Surveillance for jugular venous thrombosis in astronauts. *Vasc. Med* **27**, 365–372 (2022).
- Mokri, B. The Monro-Kellie hypothesis: applications in CSF volume depletion. *Neurology* **56**, 1746–1748 (2001).
- Mhatre, S. D. et al. Neuro-consequences of the spaceflight environment. *Neurosci. Biobehav. Rev.* **132**, 908–935 (2022).
- Streitbürger, D.-P. et al. Investigating structural brain changes of dehydration using voxel-based morphometry. *PLoS One* **7**, e44195 (2012).
- Almudayni, A. et al. Magnetic resonance imaging of the pulsing brain: a systematic review. *MAGMA* **36**, 3–14 (2023).
- Morgan, W. H. et al. Cerebrospinal fluid pressure and the eye. *Br. J. Ophthalmol.* **100**, 71–77 (2016).
- Dobrocky, T. et al. Assessing Spinal Cerebrospinal Fluid Leaks in Spontaneous Intracranial Hypotension With a Scoring System Based on Brain Magnetic Resonance Imaging Findings. *JAMA Neurol.* **76**, 580–587 (2019).
- Cronin, C. G. et al. CT evaluation of Chamberlain's, McGregor's, and McRae's skull-base lines. *Clin. Radiol.* **64**, 64–69 (2009).
- Puonti, O. et al. Accurate and robust whole-head segmentation from magnetic resonance images for individualized head modeling. *NeuroImage* **219**, 117044 (2020).
- Friston, K., Ashburner, J., Kiebel, S., Nichols, T. & Penny, W. *Statistical Parametric Mapping: The Analysis of Functional Brain Images*. (Wellcome Department of Imaging Neuroscience, 2003).
- Fedorov, A. et al. 3D Slicer as an image computing platform for the Quantitative Imaging Network. *Magn. Reson Imaging* **30**, 1323–1341 (2012).
- Boynton, R. *How to Calculate Mass Properties (An Engineer's Practical Guide)* (Raptor Scientific, 2001).
- Barratt, M. R. Physical and Bioenvironmental Aspects of Human Space Flight. in *Principles of Clinical Medicine for Space Flight* (eds. Barratt, M. R. & Pool, S. L.) 3–26 (Springer, New York, NY, 2008).
- Jenkinson, M., Beckmann, C. F., Behrens, T. E. J., Woolrich, M. W. & Smith, S. M. FSL. *Neuroimage* **62**, 782–790 (2012).
- R Core Team. R: A Language and Environment for Statistical Computing. R Foundation for Statistical Computing, Vienna, Austria (2024). Available at <https://www.R-project.org/>.
- Wickham, H. *ggplot2: Elegant Graphics for Data Analysis* (Springer-Verlag, New York, 2016). Available at <https://ggplot2.tidyverse.org>.
- Seg3D: Volumetric Image Segmentation and Visualization. University of Utah. <http://www.sci.utah.edu/cibc-software/seg3d.html> (accessed Apr 2025).

Acknowledgements

This study was supported by grant 80NSSC22K0023 through the Human Research Program of the National Aeronautics and Space Administration (NASA).

Author contributions

Concept and design: Warthen, Sater, Macias, Laurie, Martin. Acquisition, analysis, or interpretation of data: all authors. Drafting of the manuscript: Warthen, Martin. Critical revision of the manuscript for important intellectual content: all authors. Statistical analysis: Young, Warthen. All authors have read and approved the final version of this manuscript.

Competing interests

The authors declare no competing interests.

Additional information

Supplementary information The online version contains supplementary material available at <https://doi.org/10.1038/s41526-025-00468-x>.

Correspondence and requests for materials should be addressed to Bryn A. Martin.

Reprints and permissions information is available at <http://www.nature.com/reprints>

Publisher's note Springer Nature remains neutral with regard to jurisdictional claims in published maps and institutional affiliations.

Open Access This article is licensed under a Creative Commons Attribution-NonCommercial-NoDerivatives 4.0 International License, which permits any non-commercial use, sharing, distribution and reproduction in any medium or format, as long as you give appropriate credit to the original author(s) and the source, provide a link to the Creative Commons licence, and indicate if you modified the licensed material. You do not have permission under this licence to share adapted material derived from this article or parts of it. The images or other third party material in this article are included in the article's Creative Commons licence, unless indicated otherwise in a credit line to the material. If material is not included in the article's Creative Commons licence and your intended use is not permitted by statutory regulation or exceeds the permitted use, you will need to obtain permission directly from the copyright holder. To view a copy of this licence, visit <http://creativecommons.org/licenses/by-nc-nd/4.0/>.

© The Author(s) 2025